

03

N78-28 104  
III

JPL PUBLICATION 78-34

Part 2

# Computer Image Processing — Geologic Applications

23890

RECEIVED

JUN 05 1979

SIS/902.6

National Aeronautics and  
Space Administration

Jet Propulsion Laboratory  
California Institute of Technology  
Pasadena, California

JPL PUBLICATION 78-34

# Computer Image Processing — Geologic Applications

Michael J. Abrams

June 1, 1978

National Aeronautics and  
Space Administration

**Jet Propulsion Laboratory**  
California Institute of Technology  
Pasadena, California

## PREFACE

The work described in this report was performed by the Earth and Space Sciences Division of the Jet Propulsion Laboratory.

## ABSTRACT

Computer image processing of digital data was performed to support several geological studies. The specific goals were to (1) relate the mineral content to the spectral reflectance of certain geologic materials, (2) determine the influence of environmental factors, such as atmosphere and vegetation, and (3) improve image processing techniques.

For detection of spectral differences related to mineralogy we found the technique of band ratioing to be the most useful. Ratio pictures exaggerate subtle color differences and, to the first order, suppress albedo differences due to topography.

The influence of atmospheric scattering and methods to correct for the scattering were also studied. Two techniques were used to correct for atmospheric effects: (1) dark object subtraction, (2) normalization by use of ground spectral measurements. Of the two, the first technique proved to be the most successful for removing the effects of atmospheric scattering.

Finally, a digital mosaic was produced from two side-lapping Landsat frames. The advantages were that the same enhancement algorithm can be applied to both frames, and there is no seam where the two images are joined. Disadvantages included the time-consuming process of doing the mosaicking and the fact that the enhancement algorithms may not be optimal for both scenes, but are a compromise.



## CONTENTS

I.	INTRODUCTION -----	1-1
II.	COMPUTER PROCESSING PROCEDURES -----	2-1
	A.    PRELIMINARY PROCESSING -----	2-1
	B.    CONTRAST STRETCHES AND OTHER DATA DISPLAY TECHNIQUES	2-1
III.	ATMOSPHERIC CORRECTIONS -----	3-1
IV.	PLAYBACK DEVICES -----	4-1
V.	DIGITAL IMAGE MOSAICS -----	5-1
VI.	SUMMARY -----	6-1
	REFERENCES -----	7-1

### Figures

2-1.	Landsat Image and PDF; Raw, Unstretched Data -----	2-2
2-2.	Same scene as Figure 2-1; Linear Contrast Stretch Applied to Enhance Data -----	2-4
2-3.	Plots of Input DN vs Output DN for Linear, Cumulative Distribution Function and Gaussian Contrast Stretches for Figures 2-2, 2-4, and 2-5 ----	2-5
2-4.	Same Scene as Figure 2-1; Cumulative Distri- bution Function Stretch Applied to Increase Contrast -----	2-6
2-5.	Same Scene as Figure 2-1; Gaussian Stretch Applied to Data -----	2-7
2-6.	Color Additive Composite of Tintic Mountains, Utah; Linear Contrast Stretch Applied to Bands 4, 5, and 7 Prior to Color Reconstruction -----	2-9
3-1.	Goldfield, Nevada, Color Ratio Composite; Band Ratios 4/5, 5/6, and 6/7 Displayed as Blue, Green, and Red, Respectively -----	3-3

- 3-2. Goldfield, Nevada, Color-Infrared Composite  
with Correction for Atmospheric Scattering Using  
Field Reflectance Measurements to Determine  
Values ----- 3-9
- 3-3. Goldfield, Nevada, Color Ratio Composite Using  
Band Ratios 4/5, 5/6, and 6/7 Displayed as Blue,  
Green, and Red, Respectively ----- 3-11
- 5-1. Digital Mosaic of the Walker Lake Area; Color Ratio  
Composite, Band Ratios 4/5, 5/6, 6/7 Displayed  
as Blue, Green, and Red, Respectively ----- 5-3

#### Tables

- 3-1. Landsat DN Values for Darkest Object in Scene ----- 3-5
- 3-2. Landsat DN Values and PFRS Determined Albedos for  
Ground Sites ----- 3-7

## SECTION I

### INTRODUCTION

Computer image processing of digital data is performed to prepare an image for display and interpretation, or to aid in the extraction of information from the image. The goal is to improve image quality; hence it is often referred to as image enhancement. Because image quality is a subjective measure, there are no simple rules which may be followed to produce a single best image. Often several pictures made from the original image are necessary to display the information required by the analyst, and this may represent only a fraction of the total usable information contained in the original data. Thus an enhanced image may contain less information than the original image. However, a properly enhanced picture optimally displays the information that is of greatest interest to the analyst.

This philosophy has provided the guiding rationale for the image processing performed in this study. The specific goals are to (1) relate the mineral content to the spectral reflectance of certain geologic materials (2) determine the influence of environmental factors, such as atmosphere and vegetation and (3) improve image processing techniques.

The relationship between mineral composition and spectral reflectance of hydrothermally altered and unaltered materials was studied by analyzing both laboratory mineralogical determinations and spectral reflectance measurements using JPL's Portable Field Reflectance Spectrometer (PFRS) (Goetz and others, 1975, Reference 1). These studies are described in more detail elsewhere (Reference 2).

Determining the influence of environmental factors on the spectral behavior of materials has required a close collaboration between field measurements and observations and image processing procedures. Two of the factors studied in detail are the influence of vegetation on the spectral reflectance characteristics of altered materials and the effect of atmospheric scattering on reflectance recorded by the Landsat Multispectral Scanner.

The goal of improving image processing techniques is an interactive task requiring communication between the analyst and the computer programmer. The analyst specifies what part of a scene is of importance, and the programmer devises ways to process the raw data to display that part of the data. After the analyst examines and evaluates the processed image, he makes suggestions for improvement. By this iterative process, two specialists in different fields apply their expertise to a problem requiring an interdisciplinary solution. Image processing applied to geology has expanded into a viable research program as a result of the availability and quantity of Landsat digital data. Our efforts have concentrated on the extraction and display of spectral, rather than spatial, information.

Our previous studies have resulted in numerous publications, two of which provide a strong foundation for this report. Goetz and others (1975) present a detailed description of image processing techniques

applied to geological problems, including lithologic identification and mapping and hydrologic studies. In addition, the reader will find detailed sections on image processing algorithms and their application. Rowan and others (1974, Reference 3) present a thorough treatment of the image processing techniques referred to as band ratioing and its application to the detection of hydrothermally altered rocks in a well-exposed south-central Nevada study area.

These papers are representative of many in the literature concerned with enhancement techniques. However, other techniques exist and deserve mention. A large group of analysis techniques are generally referred to as classification. Classification is the process of recognizing classes or groups whose members have certain characteristics in common. The process of determining the classes can be supervised or unsupervised. In the former case, an analyst specifies training areas which are believed to be representative of the units of interest; in the latter case, the data itself is used to suggest natural categories. The elements (or in this case pixels) are then assigned by the computer to the category they most closely resemble.

Although classification techniques have been used successfully in a few geological studies (Schmidt, 1973, Reference 4), most attempts have been hampered by the inhomogeneity of most geologic units, confusing influence of vegetation and soil cover, gradational boundaries and, possibly, lack of sufficient information in the limited wavelength regions available to date (Siegal and Abrams, 1976, Reference 5). In addition, thematic classification maps lack the textural or spatial information that is so valuable for interpreting an image.

## SECTION II

### COMPUTER PROCESSING PROCEDURES

#### A. PRELIMINARY PROCESSING

Computer processing of Landsat data begins with acquisition of computer compatible tapes (CCT's). Data on the CCT's is in a band-interleaved format, uncorrected for geometric distortions. Preliminary processing of the data involves:

- (1) De-interleaving the raw data so that a Landsat image of each spectral band is stored as a separate image.
- (2) Rescaling the data from 7-bit (bands 4, 5, and 6) and 6-bit (band 7) to 8-bit bytes. This is done for convenience of later processing, as the IBM computer used at JPL operates on 8-bit words.
- (3) Geometric rectification to remove skewing of the image. Skew is caused by the rotation of the Earth during the 25 secs required for Landsat to scan a single frame. Typically, this skew is about  $3^{\circ}$ , but varies with latitude.
- (4) Correction of band-to-band misregistration and removal of synthetic pixels. Band-to-band misregistration occurs because samples from successive lines in a single channel are acquired one-twelfth of the dwell time apart; consequently each line within a six-line swath must be offset to the east by one-twelfth sample from the preceding line. Changes in the period of the oscillating scan mirror result in a different number of samples per scan. On the CCT we receive, the number of samples has been adjusted by insertion of "synthetic" pixels, which are assigned the DN (digital number) of their neighbors. These synthetic pixels are removed and the sample scale normalized by interpolation.
- (5) Resampling of rectangular pixels to square pixels. This is done to accommodate the format of the photographic playback devices, which produce pixels having a unity aspect ratio (ratio of horizontal scale to vertical scale). At this point the data is ready for further processing, display, and analysis.

#### B. CONTRAST STRETCHES AND OTHER DATA DISPLAY TECHNIQUES

A convenient statistical measure of information in an image is the probability density function (PDF), which describes the probability of finding a gray level value or DN of a given value in a picture. The PDF is displayed as a histogram, with DN values along one axis and number of pixels as the other axis. The histogram thus indicates the frequency of occurrence of gray levels over the entire image examined (Figure 2-1).

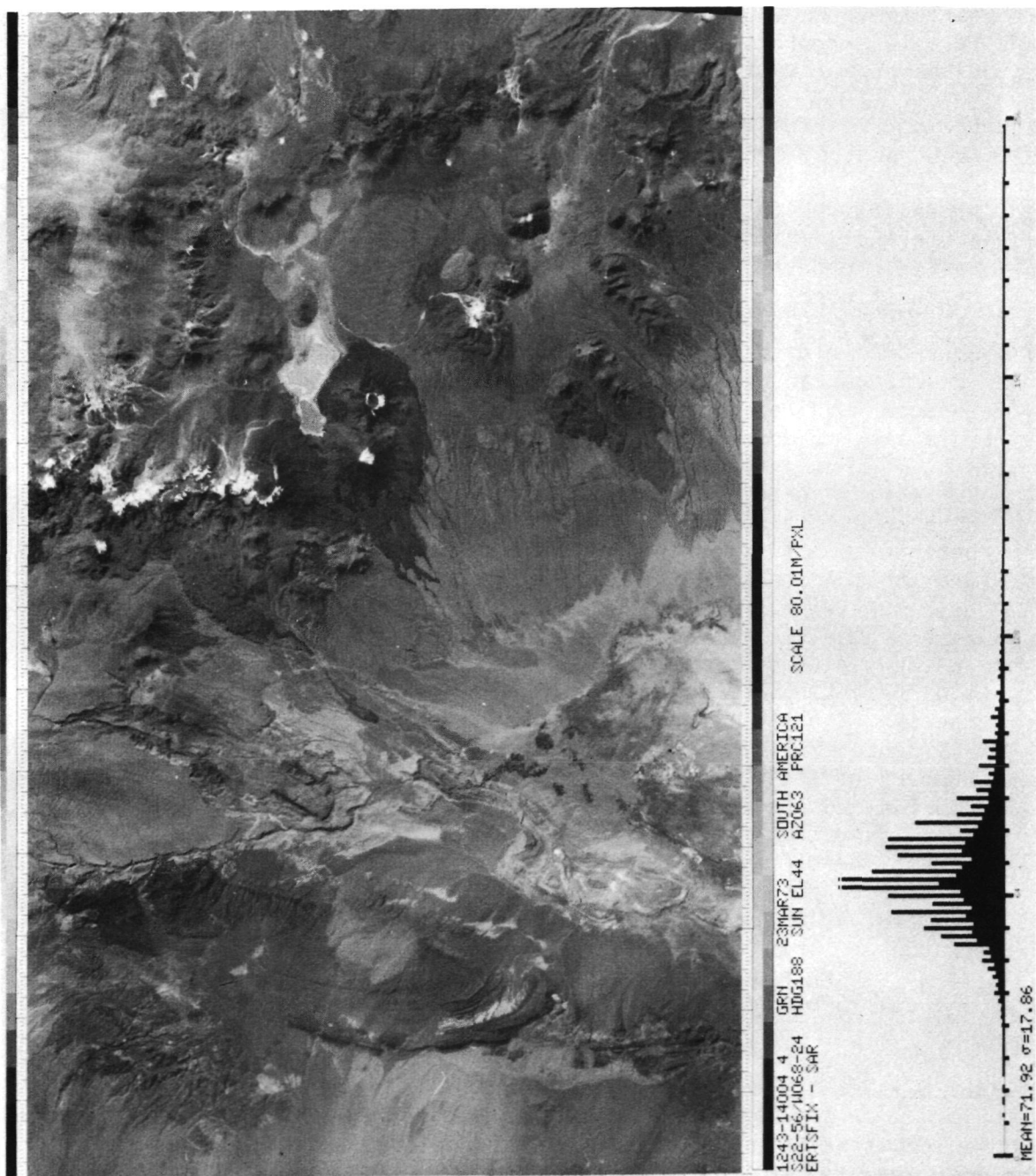


Figure 2-1. Landsat Image and PDF; Raw, Unstretched Data

Gray level distribution reveals a great deal of information about an image. A scene of a homogeneous area with low contrast will have a PDF with a single sharp peak and resemble the shape of a Gaussian distribution. Images which have more than a single type of terrain will usually have more than one peak, or a broader distribution.

Programs that modify the contrast within an image (contrast stretches) use the PDF as a necessary input. The simplest type of contrast stretch is a linear stretch:

$$DN_0 = a DN_i + b$$

where  $DN_0$  is the output DN,  $DN_i$  is the input DN, and  $a$  and  $b$  are constants defining gain and offset, respectively. This type of stretch is used to produce data which fills the dynamic range of the output playback device. Because most Landsat MSS PDF's are rather narrow, gains of about 5-10 are typically applied to the input DN's to increase contrast for display (Figure 2-2).

Linear contrast stretches can also be examined by plotting input DN versus output DN (Figure 2-3). The slope of the line is the gain, and the x-intercept is the offset. Gain is a multiplicative factor applied to increase the spread of the data; i.e., raw data having a range of 0 to 64 DN is multiplied by a gain of 4 to rescale the data to 0 to 255 DN to fill the entire dynamic range of the playback device. The offset is applied to center the rescaled distribution around DN 128, mid-gray.

Another commonly used transformation is the cumulative distribution function (CDF):

$$CDF(n) = \sum_{DN=0}^n P(DN)$$

where  $P$  is the probability of occurrence of a given DN in an image, and  $n$  is a DN within the dynamic range. The CDF of the stretched picture is forced to resemble a ramp; then each gray level in the output picture has equal numbers of pixels (Figures 2-3 and 2-4).

In practice, any mathematical function which can be defined can be used to transform the digital data. Other commonly used transformations are Gaussian (Figures 2-3 and 2-5), logarithmic, cubic, etc. (Goetz and others, 1975). All have as their goal to increase the contrast of an image or part of an image for improved display.

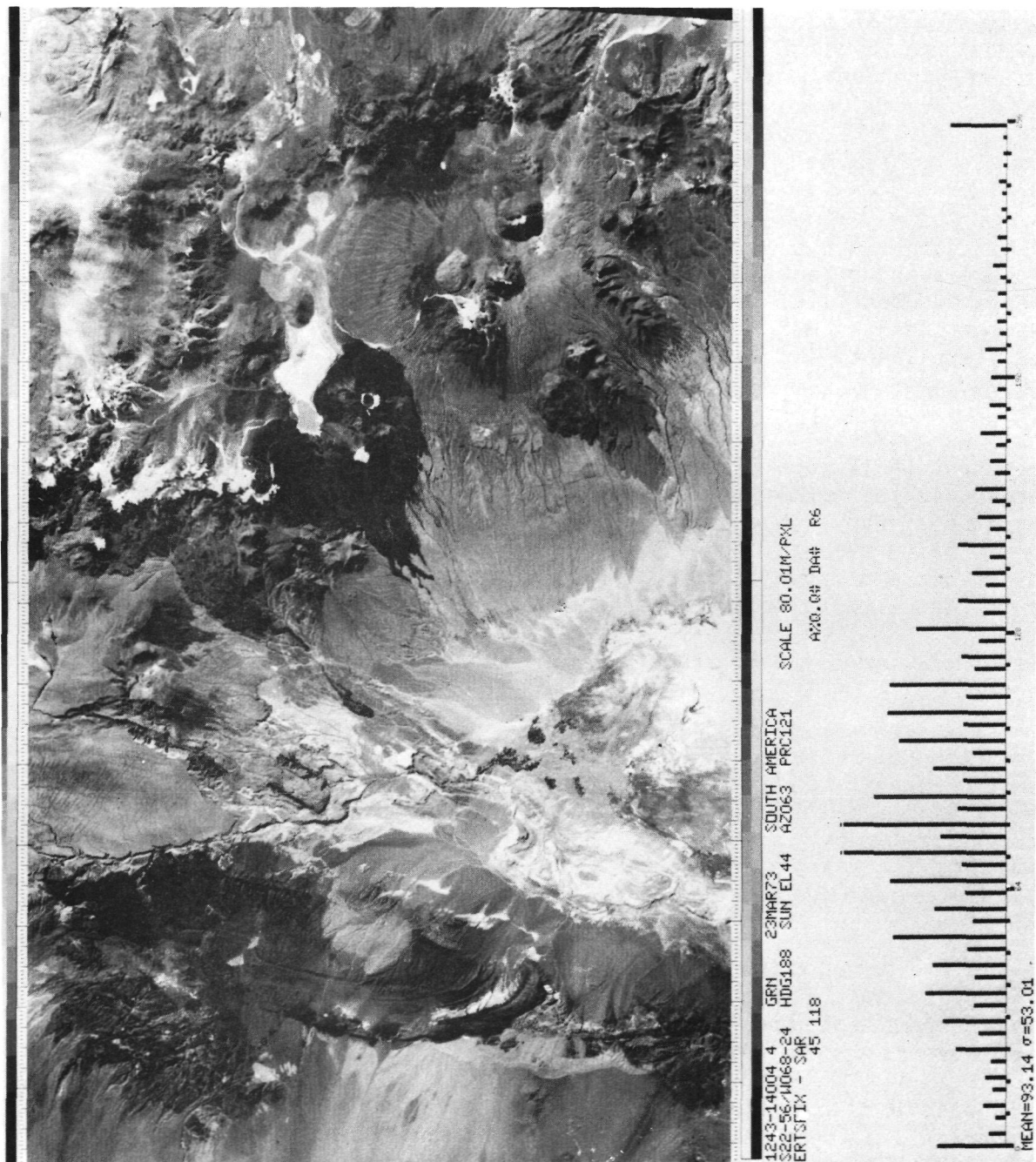


Figure 2-2. Same Scene as Figure 2-1; Linear Contrast Stretch Applied to Enhance Data (Same scale as Figure 2-1)



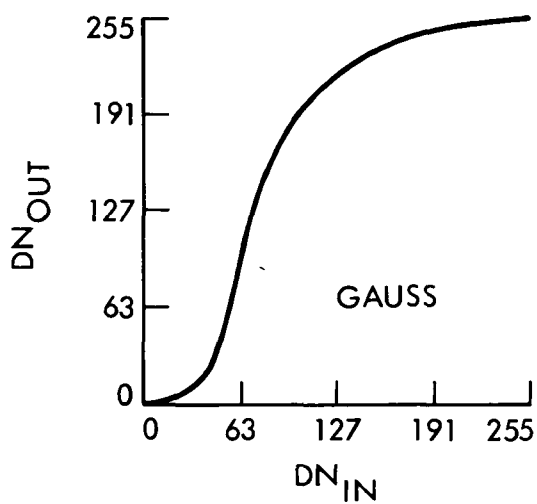
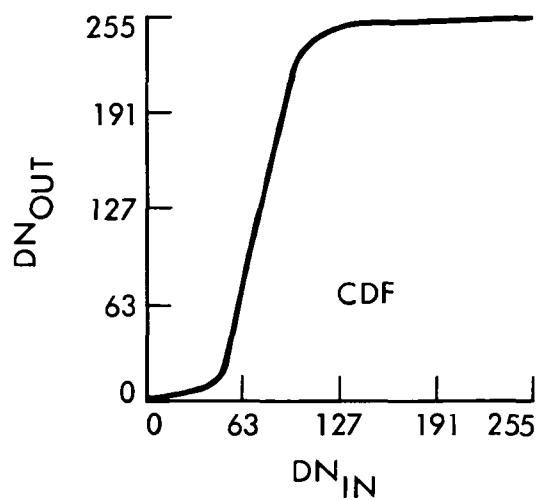
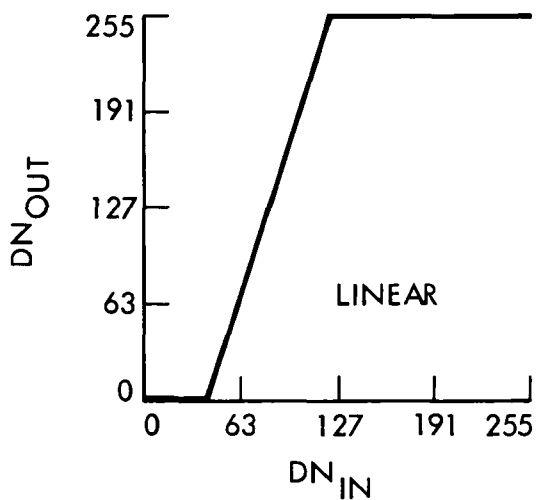


Figure 2-3. Plots of Input DN vs Output DN for Linear, Cumulative Distribution Function and Gaussian Contrast Stretches for Figures 2-2, 2-4, and 2-5

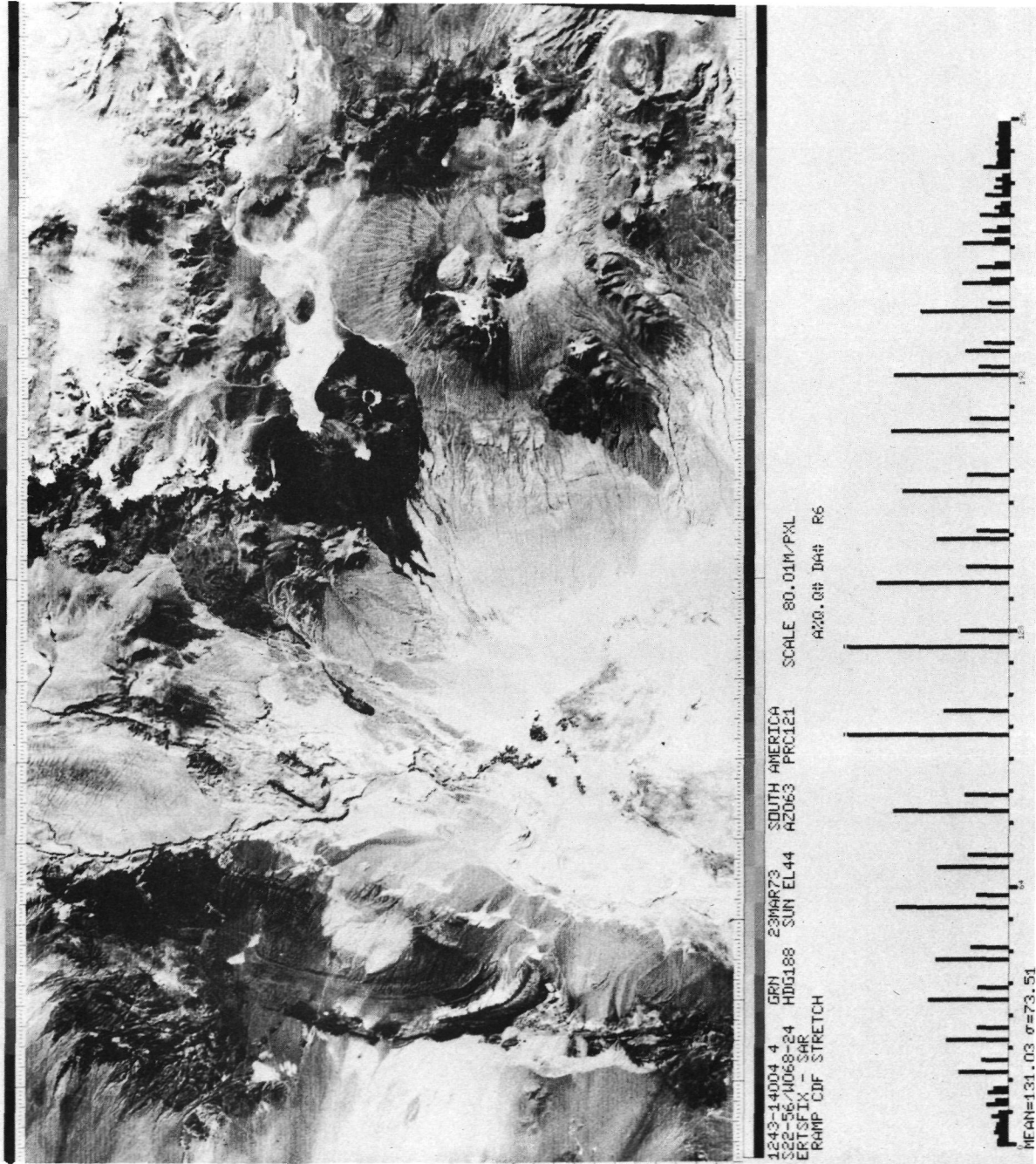


Figure 2-4. Same Scene as Figure 2-1; Cumulative Distribution Function Stretch Applied to Increase Contrast (Same scale as Figure 2-1)

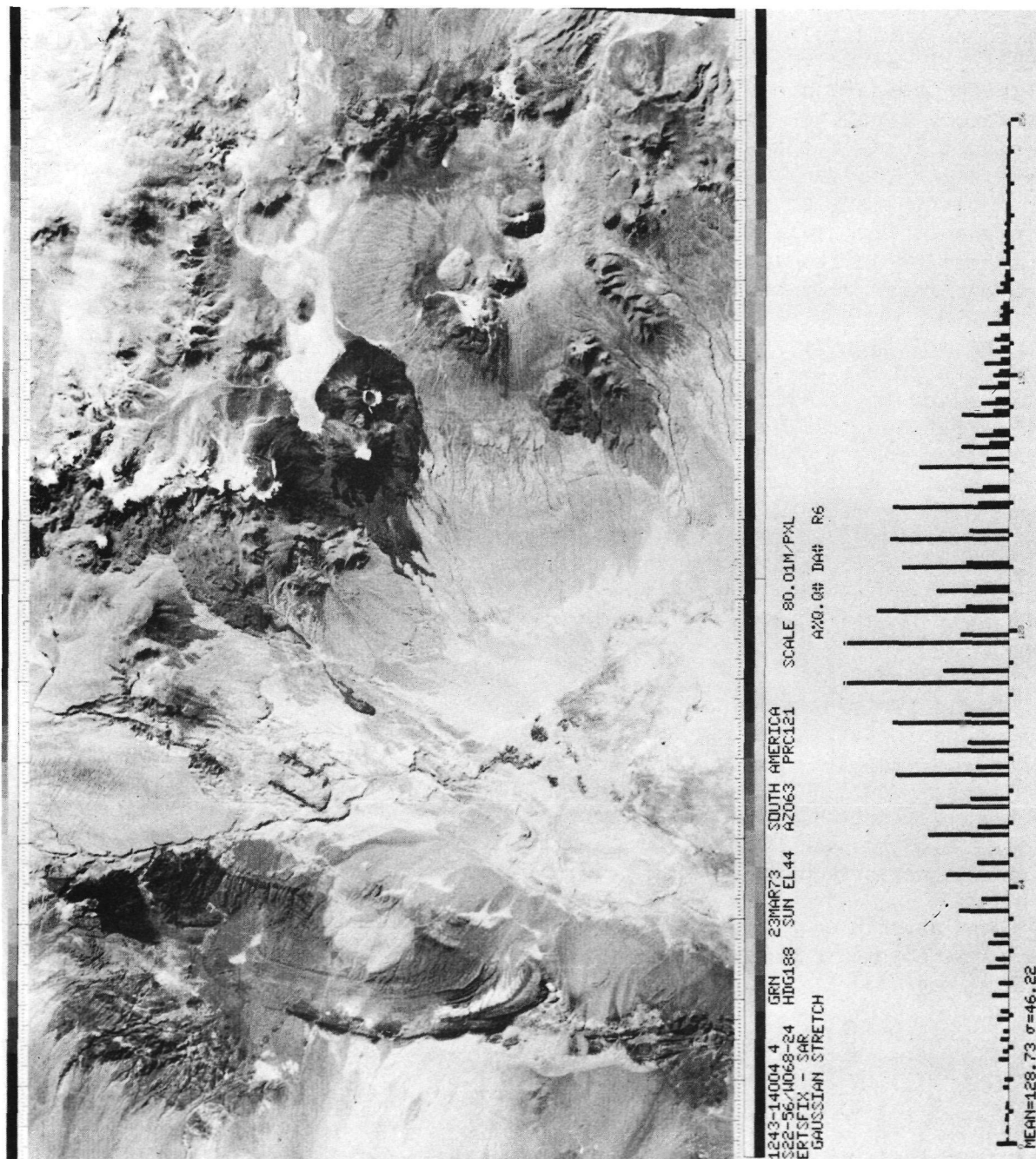


Figure 2-5. Same Scene as Figure 2-1, Gaussian Stretch Applied to Data  
 (Same scale as Figure 2-1)

All of the contrast stretch programs used at the JPL Image Processing Laboratory can be implemented in two modes: automatic and user-controlled. In the automatic mode, only a saturation level is specified. For example, a linear contrast stretch with 8% saturation would assign 4% of the input data to black (0 DN), 4% to white (255 DN) and perform a linear stretch of the remaining 92% of the data between 0 and 255. This program operates by examining the scene PDF to determine the saturation limits. For a scene whose initial PDF is normally distributed, this type of stretch will center the mode of the data at DN 128 and will symmetrically distribute the data about this value. This will usually produce a satisfactory stretch. However, a scene whose PDF is markedly skewed will result in an output image with the majority of the data either too bright or too dark. An example of this phenomenon is a scene containing water bodies, where an automatic stretch would assign DN's representing land areas to high values and water to low. If the analyst were interested in information in the land, this area would be displayed with low contrast and appear relatively bright.

The solution to this problem is to tailor the stretch to accommodate the desires of the analyst. By examination of the original PDF, DN's corresponding to water can all be assigned to zero DN, and the remaining values stretched to fill the dynamic range. In this way, land area would appear with a wide range of contrasts, and information would be more easily distinguished.

Figure 2-6 presents an example of linear contrast enhancement performed to bring out detail in vegetated mountainous areas as well as bright alluvial and bedrock areas. This process has also been extensively used for processing individual Landsat bands as well as ratio images.

The color picture shown in Figure 2-6 is a color additive composite. It was constructed by taking three black and white positive film transparencies (bands 4, 5, and 7), and pin registering them to each other. Each transparency was then used to expose a sheet of color negative material, sequentially exposing one band in blue light, the second in green light, and the third in red light. The color negative was then developed and prints were produced from it.

For detection of spectral difference we have found the technique of band ratioing to be the most useful. The algorithm used to construct a ratio image is

$$DN_0 = a \frac{DN_1}{DN_2} + b$$

where  $DN_0$  is the output DN,  $DN_1$  and  $DN_2$  are input DN's of two channels, and a and b are constants required to scale the ratio information, which can range from 0 to  $\infty$ , to 256 gray levels for storage and display. In most Landsat images the ratios are centered about 1.





Figure 2-6. Color Additive Composite of Tintic Mountains, Utah; Linear Contrast Stretch Applied to Bands 4, 5, and 7 Prior to Color Reconstruction (Scene 1735-17335)

**Page Intentionally Left Blank**

Ratio pictures are useful because they exaggerate spectral differences. If the albedo or the illumination changes across the scene, but the spectral reflectance does not, the ratio picture will show no change. Ratio pictures have the effect of suppressing the detail which is caused by topographic effects, while emphasizing spectral reflectance boundaries. This occurs because a ratio picture is essentially an image of the slope of the spectral curves of the materials in the scene between the two wavelengths used in the ratio. However, ratioing suppresses the ability to discriminate between rocks with strikingly different albedo, but similar shapes of spectral reflectance curves (for instance some dark basalts and light marls).

2-10 Blank



### SECTION III

#### ATMOSPHERIC CONDITIONS

The presence of the atmosphere and varying illumination conditions on the brightness ( $K_x$ ) perceived at a spacecraft is given by:

$$K_x = G_x P_x \phi + N_x$$

where  $x$  denotes the wavelength band;  $G$  is a factor containing the solar irradiance, atmospheric transmittance and instrument response;  $P$  is the bidirectional spectral reflectance;  $\phi$  is a photometric function dependent on the azimuth angle between the slope and the sun and on the angle between the spacecraft and the satellite; and  $N$  is the path radiance or contribution from the scattered light in the intervening atmosphere (Rowan, and others, 1977, Reference 6).

The additive term  $N_x$  can be estimated in several ways. For instance, (1) assuming that the brightness of the darkest objects in the scene (deep, clear water, cloud shadows, or very dark material) is due solely to atmospheric scattering, and using the DN value as a correction; (2) determining absolute reflectance values on the ground and then normalizing the radiances measured by the satellite.

Using the first method, Goetz and others (1975) found by measuring the brightness of uniform material within and outside cloud shadow that  $N_x$  ranged from 24 to 10 DN as a function of the wavelength band.

In the present study a different approximation referred to as "dark object subtraction" (DOS) was used. By examination of the PDF's for the four Landsat bands for Goldfield, Nevada (Scene 1072-18001), the darkest materials in the scene were identified, with corresponding DN's given in Table 3-1.

These numbers were used in the modified ratio equation:

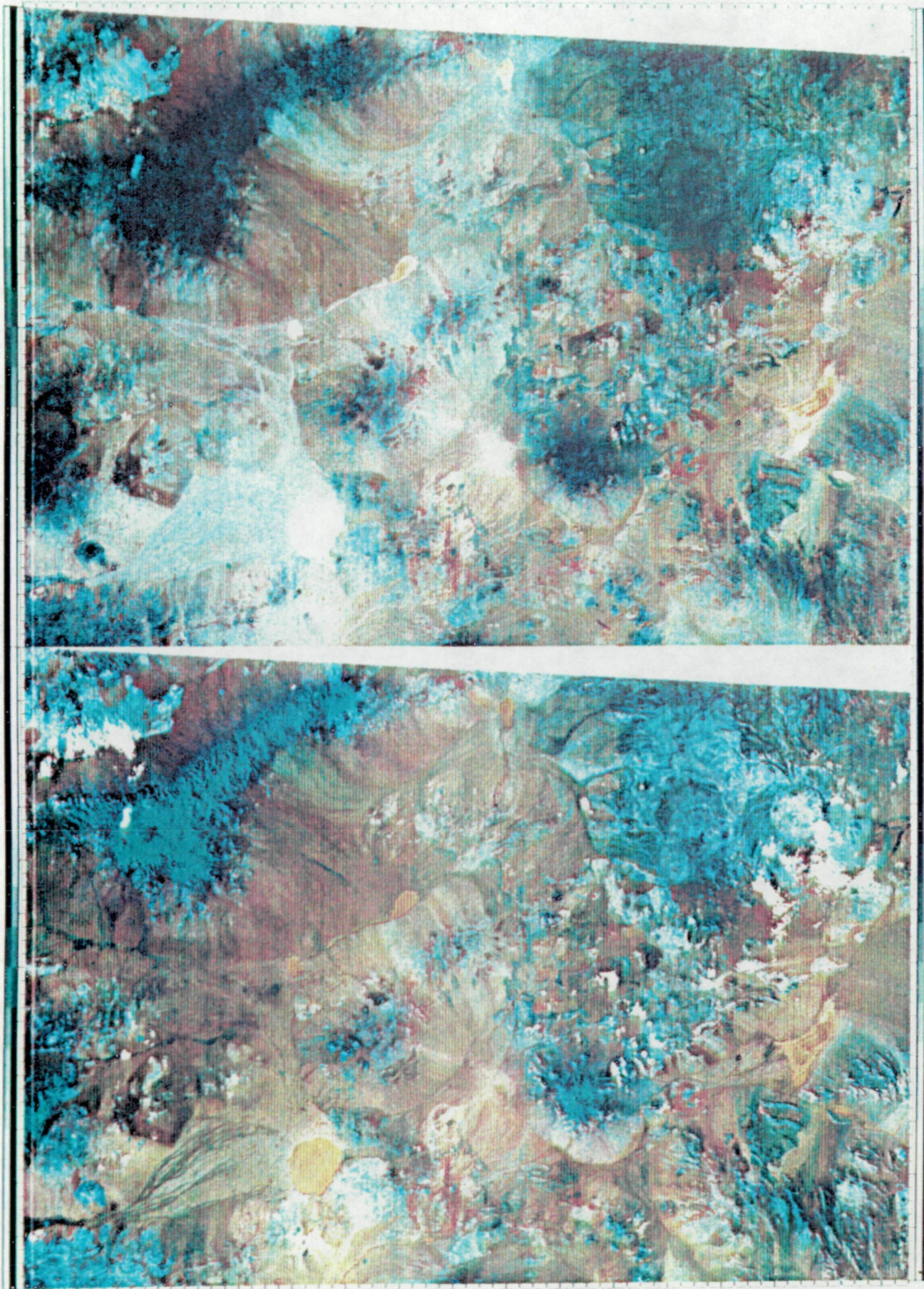
$$DN_0 = a \frac{DN_{1-atm_1}}{DN_{2-atm_2}} + b$$

where 1,2 are two wavelength channels, and  $atm_1$  and  $atm_2$  are the DN's that the sensors would record if they received only light scattered from the sky. Black-and-white ratio images 4/5, 5/6, and 6/7 were produced and used to produce a color-ratio composite (CRC). Figure 3-1 shows this ratio composite before (A) and after (B) dark object subtraction. Examination of the CRC without DOS indicates that a substantial amount of topographic information remains in the scene. After DOS, most of the topographic detail has been removed and spatial information lost.



**Page Intentionally Left Blank**





1054-18001 GOLDFIELD, NEVADA  
 107-58 117-25 M06190 0300172  
 107-58 117-25 M06190 0300172  
 ROTID = FSC 4.0 = SCALE 79.95M/42  
 STRETCH = FSC 4.0 = 155 - INSECT  
 LINEAR STRETCH, PERC 8.0

Figure 3-1. Goldfield, Nevada, Color Ratio Composite; Band Ratios 4/5, 5/6, and 6/7 Displayed as Blue, Green and Red, Respectively (A, without dark object subtraction; B, with dark object subtraction. Scene 1054-18001)

3-2 Blank



**Page Intentionally Left Blank**

Table 3-1. Landsat DN Values for Darkest Object in Scene

	Band			
	4	5	6	7
DN of darkest object	24	10	6	1

In theory this is a desirable result, but in practice the loss of spatial information can be disturbing to the analyst. On the other hand, analysis of the DOS ratio composite indicates that additional information is displayed in areas with high relief (and shadowing); e.g., along the southwestern edge of the Kawich Range (upper right corner of image) orange colors indicative of possible alteration are now discernible.

It should be pointed out that this method provides only approximate values for  $N_x$ . In reality, the DOS terms are too large, as the radiance from the darkest objects in the scene is due to both atmospheric scattering and some small non-zero reflectance value.

A more exact approach was tried by normalizing the same Landsat scene to absolute brightness by use of field-acquired reflectance data. JPL's Portable Field Reflectance Spectrometer was used to acquire reflectance spectra for pixel-sized areas in the region of Goldfield. In practice this was accomplished by sampling an area on an 8 x 8 grid at 10 m spacings, then determining an average spectrum for each area based on 64 individual spectra. The PFRS records a bidirectional reflectance spectrum normalized to a Fiberfrax standard. This spectrum was then normalized to MgO and finally to absolute reflectance:

$$R(\nu) = \frac{R_m}{FF} \times \frac{FF}{MgO} \times MgO_a$$

where  $R_m$  is the measured reflectance of the sample, FF is the reflectance of Fiberfrax, MgO is the reflectance of magnesium-oxide standard, and  $MgO_a$  is the absolute reflectance of magnesium-oxide (Wendlandt and Hecht, 1966, Reference 7).

3.4 Blank

Albedo was calculated from the relationship:

$$A = \frac{\sum_{\nu} R(\nu) \Delta \nu}{\sum_{\nu} \Delta \nu}$$

where A is the albedo,  $\Delta \nu$  is the wavelength region being considered, and  $R(\nu)$  is defined above. In making this calculation it was assumed that the sensor (Landsat MSS) had perfect response in the region  $\Delta \nu$  and no response outside the region.

Six sites were sampled on the ground and spectra recorded and processed as above. The DN's for the Landsat bands were listed from the CCT's (Table 3-2) and plotted against calculated PFRS albedos. A least squares fit to the data points provided the following relationships against calculated albedos:

$$DN_4 = 396 (A) + 37.0 \quad R^2 = .98$$

$$DN_5 = 435 (A) + 19.2 \quad R^2 = .99$$

$$DN_6 = 385 (A) + 10.0 \quad R^2 = .98$$

$$DN_7 = 320 (A) + 2.8 \quad R^2 = .98$$

where  $DN_n$  is the DN value for band n and  $R^2$  is the confidence coefficient. Setting albedo equal to zero gives the contribution from the scattered light.

A false color-infrared composite (Figure 3-2) and color-ratio composite (Figure 3-3) were produced using these correction values. In the black-and-white images used to make the color-infrared composite, 0 DN (black) represents 0 albedo, and 255 DN (white) represents an albedo of 0.5. To produce the ratio picture, corrections of 37, 19, 10, and 3 DN were used in the modified ratio equation.

Comparing these correction numbers to those found from the DOS indicates that there are objects in the scene that appear to have negative albedos. The inconsistency of this conclusion can be explained by considering sources of error. The 80 x 80 m sampling areas did not correspond 1 to 1 with a single Landsat pixel. Rather the sample sites were found to overlap several (up to 4) pixels, so an average value of all overlapped

Table 3-2. Landsat DN Values and PFRS Determined Albedos for Ground Sites

Site	Band							
	4		5		6		7	
	DN	Albedo	DN	Albedo	DN	Albedo	DN	Albedo
1	168	.352	210	.461	196	.510	168	.533
2	64	.068	58	.084	52	.099	45	.111
3	58	.086	53	.106	49	.125	42	.140
4	209	.419	238	.484	212	.498	168	.496
5.	75	.078	68	.093	52	.105	36	.111
6.	84	.100	103	.188	99	.222	81	.243

pixels was used. The resulting DN value of necessity included values for areas different in composition and albedo from the spectrally sampled sites.

The sampling procedure itself probably introduced some bias, as all 64 points were not measured due to inaccessibility. Materials which produced rugged topography were therefore not sampled.

Other possible sources of errors were the assumption that the Landsat sensor response was perfect and linear, the assumption that the areas sampled by Landsat were flat, and the neglect of small non-uniform shadows in the PFRS field of view, caused by surface texture.

**Page Intentionally Left Blank**





1054-18001 180 15SEP72 GOLDFIELD, NEVADA  
 N37-23-46.17-29 HDG190 SUN EL47 AZ139 PRC121 SCALE 79.95M-PIX  
 144  
 STRETCH 23-1750

PDOX SUN PWR 6. 1977 000729 .JPL-IPL

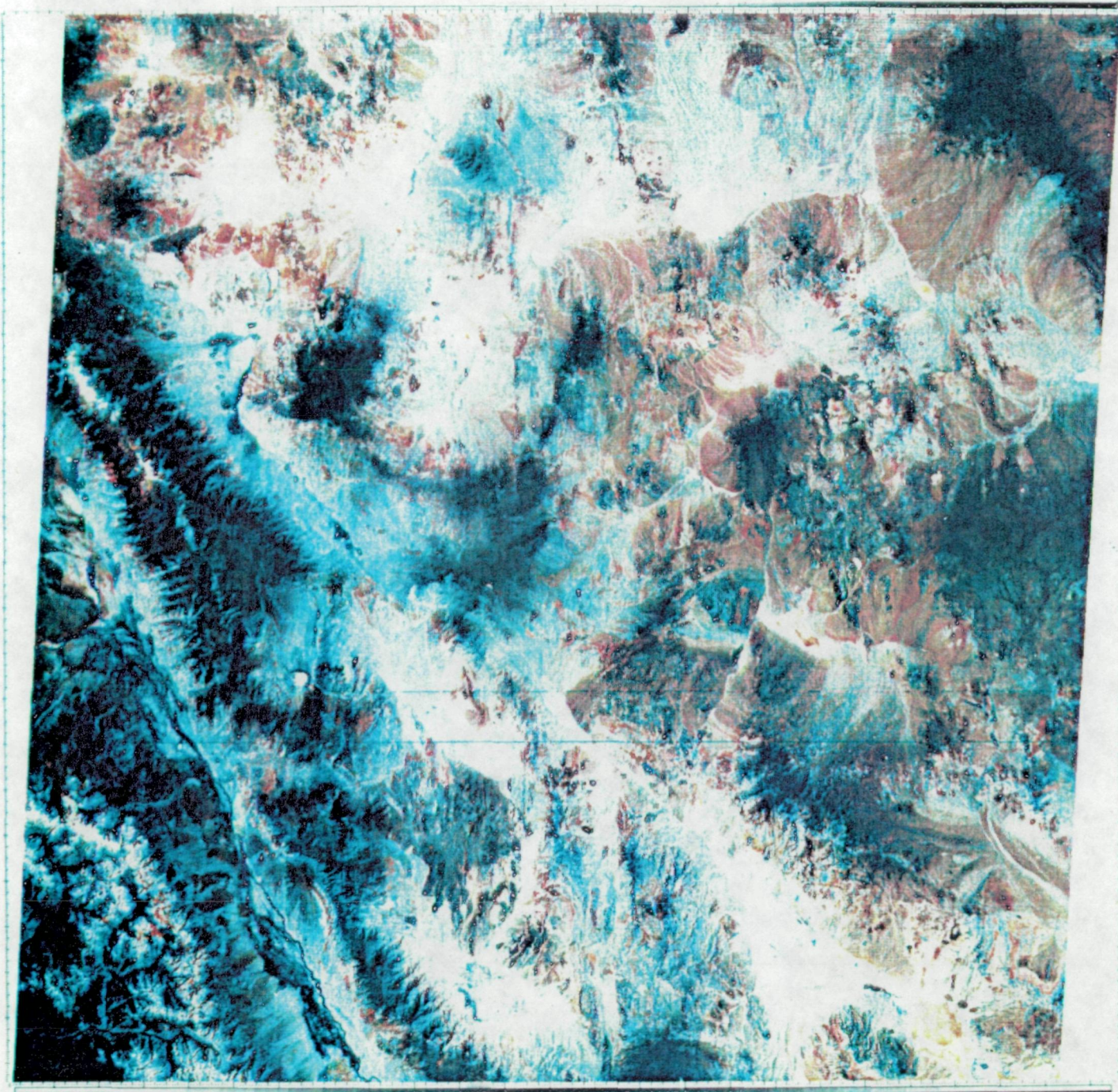
Figure 3-2. Goldfield, Nevada, Color-Infrared Composite With Correction for Atmospheric Scattering Using Field Reflectance Measurements to Determine Values (Scene 1054-18001)

38 Blank



**Page Intentionally Left Blank**





1054-18001 8 SR3 15SEP78 GOLDFIELD, NEVADA  
 R37-23-14117-29 MAG190 SUN EL47 AZ129 PRCL21 SCALE 79.95M-PIX  
 568 - F - RAMP CDF STRETCH

CALISK THU MAR 24 1977 030458 JPL IPL

Figure 3-3. Goldfield, Nevada, Color Ratio Composite Using Band Ratio 4/5, 5/6, and 6/7 Displayed as Blue, Green and Red, Respectively (Correction for atmospheric scattering included; values were determined using field reflectance measurements. CDF stretch applied. Scene 1054-18001. Note that this differs from that in Figure 2-1)

3-10 Blank



## SECTION IV

### PLAYBACK DEVICES

Processed Landsat data was converted to film products using several playback devices. Each of the devices converts the digital data from computer-compatible tape to an analog signal which modulates a light beam that is used to expose black and white negative film.

The bulk of the playback operation was performed on JPL's Video Film Converter (VFC). This device is a cathode ray tube, flying spot scanner which exposes 70-mm strip film. A variable pixel spacing allows images to be placed on the film to cover the entire usable film area. The size of the output film and images was chosen to be compatible with an additive color viewer, which accepts 70-mm film chips. By use of a table look-up procedure in the light control, film density is forced to be linear with DN and ranges from a fog level of 0.13 to a maximum density of 1.33. The pixel size is fixed, so that at most spacings, overlap or underlap of pixels results. This results in producing images which, in general, do not have optimal resolution.

For higher quality playback, images were produced on an Optronics drum plotter. This device uses a light-emitting diode (LED) to expose 8 x 10 negative material and has only three pixel spacings available: 25, 50, or 100  $\mu\text{m}$ . The advantages of using this device are greater geometric precision, single pixels in a pixel grid arrangement, and (usually) larger images. Triplets of images from the Optronics were used for color reconstruction via standard techniques.

A third device used to create images was the Geospace 34/10 drum plotter. This device produces images on 36-in. negative material at either 192, 96, or 48 lines per inch. The advantages of this larger format are that individual pixels can be easily seen, and color reconstructions made from these products do not need further enlarging to be used for detailed work. Therefore, resolution degradation from intermediate products is avoided. One disadvantage of this device is that the pixels are not square but rather have an aspect ratio of 1.0416. This required resampling the original unity aspect data to increase the number of samples per line. The resampling process used a nearest neighbor algorithm to define the new output DN's. This procedure does not degrade the image spectrum, as do convolution algorithms, because no interpolation takes place.

In the course of this project it was found that all three devices were useful for a particular phase of the work. Having the flexibility to produce first-generation products at a variety of scales allowed construction of color products with a minimum of photographic degradation caused by intermediate steps.

## SECTION V

### DIGITAL IMAGE MOSAICS

A digital mosaic of the Walker Lake Nevada area (Figure 5-1) was created using Landsat scenes 1072-18001 (Goldfield) and 1380-18111 (Comstock). The advantages of making the mosaic digitally rather than photographically were (1) there is no seam evident where the images were joined; (2) the data was still in digital form, so it could be treated as a single, large data set and computer-processed; and (3) both scenes could be processed identically to produce ratio images, contrast stretches, etc.

The mosaicking procedure first involved identifying common points in the overlap region between the two scenes (tie points) and determining the relative coordinates at the points. One scene is then selected as the base scene; the other one was forced to fit it geometrically by rubber-sheet stretching. This computer procedure uses the tie points to fit a polynomial surface to the scene being stretched, then uses interpolation to reassign pixels from the original scene to the geometrically modified scene.

In a similar fashion, overlap areas were identified, and the PDF's were forced to match by stretching one to be similar to the other. After performing these two processes, the two scenes were concatenated into a single data set and could be treated as one image.

The advantages of digital mosaicking to the analyst have been described previously. These must be weighed against the disadvantages: (1) the mosaicking process is time-consuming; (2) large digital data sets require more computer time to process. Automatic registration programs currently exist which compute cross-correlations between two areas and arrive at some "best fit." If the scenes are not very different, this procedure is much faster than the one outlined above. At the time the mosaic was created, these programs were not operable. The problem of increased computer time for processing large data sets is in fact fictitious, if both (or several) scenes were to be processed individually. An additional disadvantage is that the contrast stretch used may not be optimal for both scenes. For example, if one scene contains mostly vegetated mountains and the other arid desert regions, the stretch will be a compromise in order to display the most amount of information for both terrains. In practice this is a small sacrifice to make when weighed against the advantage of having data in both scenes displayed identically.

**Page Intentionally Left Blank**



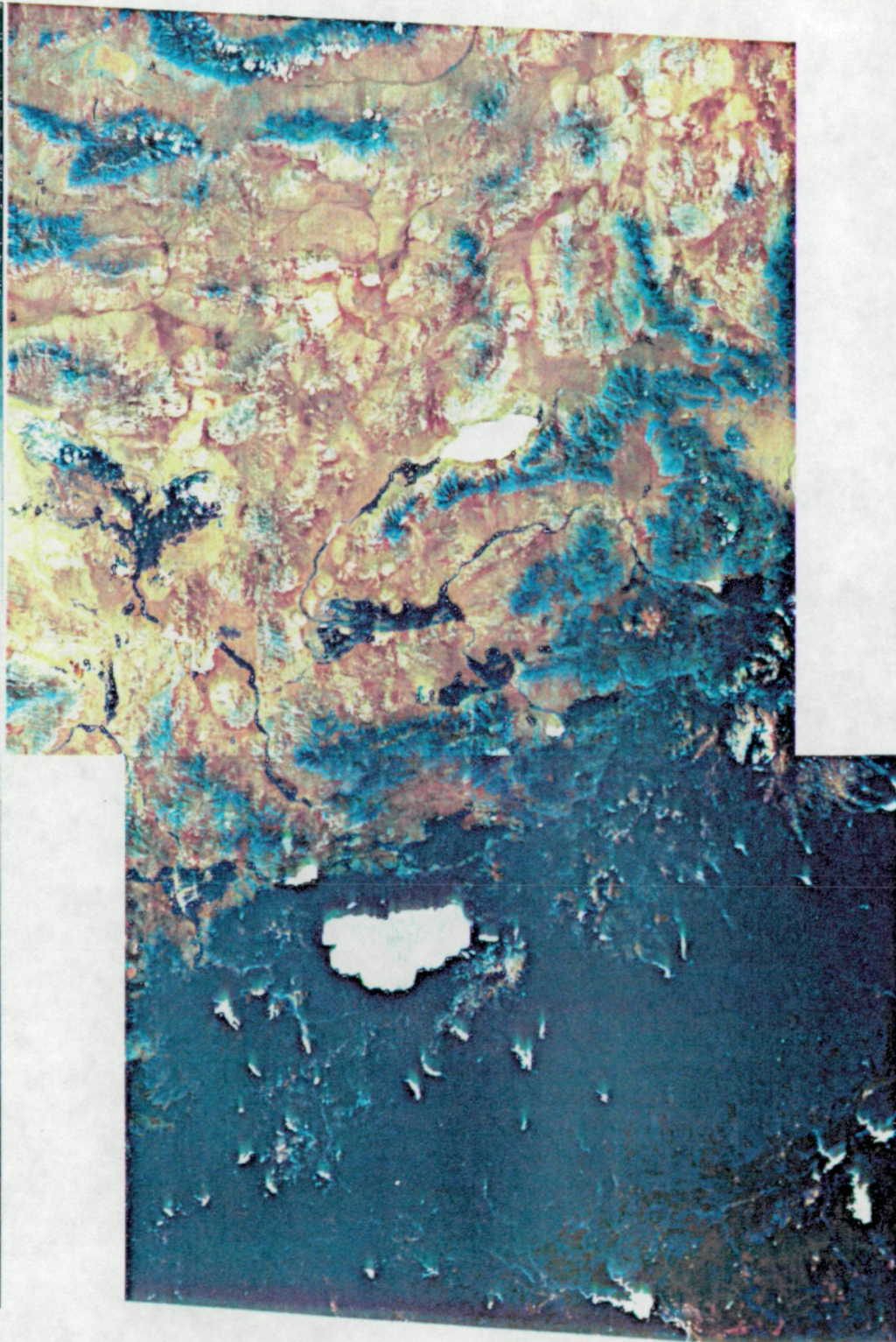


Figure 5-1. Digital Mosaic of the Walker Lake Area; Color Ratio Composite, Band Ratios 4/5, 5/6, 6/7 Displayed as Blue, Green and Red, Respectively

5-2 Blank

## SECTION VI

### SUMMARY

Computer image processing of digital data was performed to support several geological studies. The specific goals were to (1) relate the mineral content to the spectral reflectance of certain geologic materials, (2) determine the influence of environmental factors, such as atmosphere and vegetation, and (3) improve image processing techniques.

Enhancement of images requires an interaction between the analyst and the computer programmer. The analyst specifies which part of the scene or data is of importance, and the programmer devises ways to process the data to optimize the display of that part of the data. Many techniques are available for image enhancement, and several of these were described.

For detection of spectral differences related to mineralogy we found the technique of band ratioing to be the most useful. Ratio pictures exaggerate subtle color differences and, to the first order, suppress albedo differences due to topography.

The influence of atmospheric scattering and methods to correct for the scattering were also studied. Two techniques were used to correct for atmospheric effects: (1) dark object subtraction; (2) normalization by use of ground spectral measurements.

In the first method the darkest object in the scene was assumed to have zero albedo, and the reflectance values are due to atmospheric scattering only. These values were subtracted from the DN's for each band prior to ratioing or other processing. Analysis of ratio images created using this algorithm indicated that this technique effectively removed effects of atmospheric scattering (such as albedo differences due to topography and uneven illumination conditions).

The second method tried was to acquire ground-based reflectance measurements for selected, homogeneous areas. Absolute reflectances for the Landsat wavelength bands were then calculated and corrections for atmospheric scattering for corresponding Landsat pixels were determined. Analysis of ratio images created from this algorithm indicated that the technique was not successful. Large errors could be attributable to (1) the assumption that the Landsat sensor response was perfect and linear; (2) bias in the ground sampling procedure, so materials which produced rugged topography were not sampled; (3) lack of one-to-one correspondence between the ground sampled sites and the Landsat pixels.

Finally, a digital mosaic was produced from two side-lapping Landsat frames. The advantages were that the same enhancement algorithm can be applied to both frames, and there is no seam where the two images are joined. Disadvantages included the time-consuming process of doing the mosaicking and the fact that the enhancement algorithms may not be optimal for both scenes, but are a compromise.



## REFERENCES

1. Goetz, A. F. H., Billingsley, F. C., Gillespie, A. R., Abrams, M. J., Squires, R. L., Shoemaker, E. M., Lucchitta, I., and Elston, D. P., Application of ERTS Images and Image Processing to Regional Geologic Problems and Geologic Mapping in Northern Arizona, Technical Report 32-1597, Jet Propulsion Laboratory, Pasadena, California, May 15, 1975.
2. Rowan, L. C., and Abrams, M. J., "Evaluation of Landsat Multispectral Scanner Images for Mapping Altered Rocks in the East Tintic Mountains, Utah," U. S. Geological Survey Miscellaneous Investigation MI \_\_\_\_\_, 1978, in preparation.
3. Rowan, L. C., Wetlaufer, P. H., Goetz, A. F. H., Billingsley, F. C., and Stewart, J. H., "Discrimination of Rock Types and Detection of Hydrothermally Altered Areas in South-Central Nevada by the use of Computer-Enhanced ERTS Images," U.S. Geological Survey Professional Paper 883, Washington, D. C., 1974.
4. Schmidt, R. G., "Use of ERTS-1 Images in the Search for Porphyry Copper Deposits in Pakistani Baluchistan," in Symposium on Significant Results Obtained from the Earth Resources Technology Satellite-1, NASA SP-327, 1973.
5. Siegal, B., Abrams, M., "Geologic Mapping using Landsat Data," Photogrammetric Engineering and Remote Sensing, Vol. 42, No. 3, March 1976.
6. Rowan, L. C., Goetz, A. F. H., and Ashley, R. P., "Discrimination of Hydrothermally Altered and Unaltered Rocks in Visible and Near Infrared Multispectral Images," Geophysics, Vol. 42, No. 3, April 1977, pp. 522-535.
7. Wendladt, W. W., and Hect, H. G., Reflectance Spectroscopy, Interscience Publishers, New York, 1966.